ETHIOPIAN INTERNATIONAL JOURNAL OF MULTIDISCIPLINARY RESEARCH

eISSN: 2349-5715 pISSN: 2349-5707

Volume: 12, Issue 05, May-2025 SJIF 2019: 4.702 2020: 4.737 2021: 5.071 2022: 4.919 2023: 6.980 2024: 7,662

STRUCTURAL INTEGRITY OF 2024-T351 ALUMINUM ALLOY RECYCLED FROM AIRBUS A320 WING SECTIONS UNDER FATIGUE LOADING

Dustmurodov Eldor Eshbobo ugli

Tashkent State Transport University, Faculty of Aviation Transport Engineering,

Tashkent, Uzbekistan.

eldordustmurodov@mail.ru

Abstract: This study examines the residual fatigue strength of 2024-T351 aluminum alloy recovered from the decommissioned wing panels of an Airbus A320 at the end of its operational life. Fatigue performance was assessed through S-N curves and crack growth rate (da/dN) measurements, and the results were compared with those of unused (virgin) material tested under identical conditions. Fractographic analysis of fracture surfaces supported the interpretation of fatigue behavior, and fatigue life predictions were conducted using the AFGROW software. The findings provide insight into the mechanical integrity and reusability of recycled aerospace-grade aluminum alloys.

Key words: aging aircraft; fatigue crack initiation; fatigue crack propagation; fractography.

Intraduction

The global number of civil transport aircraft reaching the end of their originally specified service life is steadily increasing. Beyond considerations related to life extension, a comprehensive understanding of structural conditions at the end of service is essential for effective fleet management and the advancement of future aircraft design. In response to this need, the French national program DIAGNOSTAT was launched, supported by an interministerial fund and the Aerospace Valley competitiveness cluster. The program's primary goal was to obtain feedback on the structural state of aircraft at the end of their operational life and to develop innovative non-destructive evaluation methods for assessing this condition. While DIAGNOSTAT encompassed various material classes, including composites, this study specifically investigates the residual fatigue strength of 2024-T351 aluminum alloy, sourced from the wing panels of a decommissioned Airbus A320. Given that wing materials endure complex loading and thermal stresses, aging may significantly impact fatigue behavior [1]. However, current knowledge regarding the residual strength of such materials at the end of service remains limited, with only a few references available in the literature [2–4]. This work aims to address that gap by evaluating the end-of-life fatigue strength of the material and comparing it with data obtained from unserved (new) material using consistent testing methods.

This paper presents the main findings of the study. The potential impact of aging on fatigue life was assessed by constructing S-N curves for both new and service-exposed wing materials. A similar approach was used to evaluate the effect of real-world aging on fatigue crack growth resistance. The fatigue data obtained are supported by a fractographic analysis of the fracture surfaces.

Experimental Methods

eISSN: 2349-5715 pISSN: 2349-5707

Volume: 12, Issue 05, May-2025 SJIF 2019: 4.702 2020: 4.737 2021: 5.071 2022: 4.919 2023: 6.980 2024: 7,662

This study investigates intrados wing panels extracted from an Airbus A320 aircraft with Manufacturer Serial Number (MSN) 004. The aircraft was operated for 21 years, accumulating 38,637 flight cycles and 35,342 flight hours. Two distinct regions of the wing, illustrated in Figure 1, were analyzed. The first region, located at the wingtip, was subjected to relatively low mechanical loading, while the second, positioned near the engine, experienced significantly higher mechanical stresses.

Fig. 1: Investigated areas of the wing panels of the MSN004 A320 aircraft.

The wing panels under investigation were fabricated from laminated plates, with the grain direction running parallel to the wing's longitudinal axis. A reference sample of the new (unused) material was

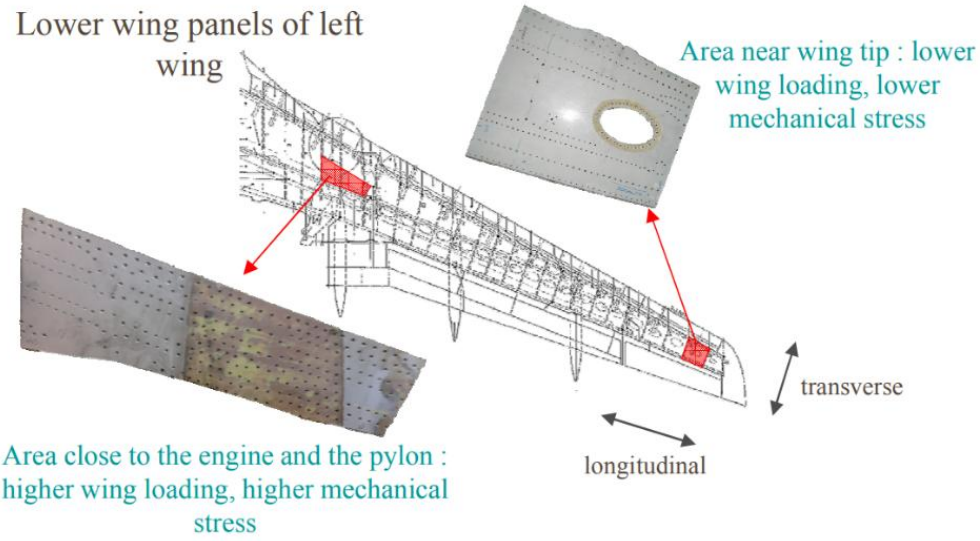

obtained from a 50 mm thick sheet for comparison purposes. Further details and fatigue performance data for this material can be found in references [5,6]. Results from tensile testing reveal that the aged material in both examined areas demonstrates higher yield strength and ultimate tensile strength than the new material. Notably, the yield strength is highest in the region near the engine, suggesting that this area may have experienced more severe aging conditions.

Fatigue testing was conducted on flat specimens with a dog-bone geometry. Prior to testing, all external surfaces were mechanically polished to achieve a surface roughness of 1 micron, minimizing the risk of early crack initiation caused by surface imperfections. Testing was carried out to failure at five applied stress levels: 250, 275, 300, 350, and 400 MPa. To evaluate the influence of grain orientation, specimens were tested in both the longitudinal (L) and transverse (T) directions. All tests were performed in laboratory air at ambient temperature, using a load ratio (R) of 0.1, and continued until complete fracture. Additionally, fatigue crack growth experiments were carried out in laboratory air using CCT W40-type specimens. These tests were conducted at a load ratio of 0.1 and a loading frequency of 20 Hz. Crack propagation was monitored optically during the tests with a traveling microscope. The outcomes are presented as plots of crack growth rate versus the range of the stress intensity factor.

Results

eISSN: 2349-5715 pISSN: 2349-5707

Volume: 12, Issue 05, May-2025 SJIF 2019: 4.702 2020: 4.737 2021: 5.071 2022: 4.919 2023: 6.980 2024: 7,662

Residual Fatigue Life. Fatigue test outcomes are displayed in Figure 2, where each data point corresponds to the average fatigue life measured across three specimens. At the selected maximum stress level, no substantial differences in fatigue life were found between the various aging conditions. However, the aged material tended to exhibit slightly longer fatigue life compared to the new material. To adjust for the differences in strength identified during tensile testing, the data were normalized by dividing the applied maximum stress by the corresponding yield strength. As shown in Figure 3, this adjustment led to a noticeable reduction in data scatter.

Fig. 2: S-N curves of wing areas A and B in the longitudinal and transverse directions compared with data obtained from the original material.

Fractographic analysis under low magnification enabled identification of crack initiation sites, which

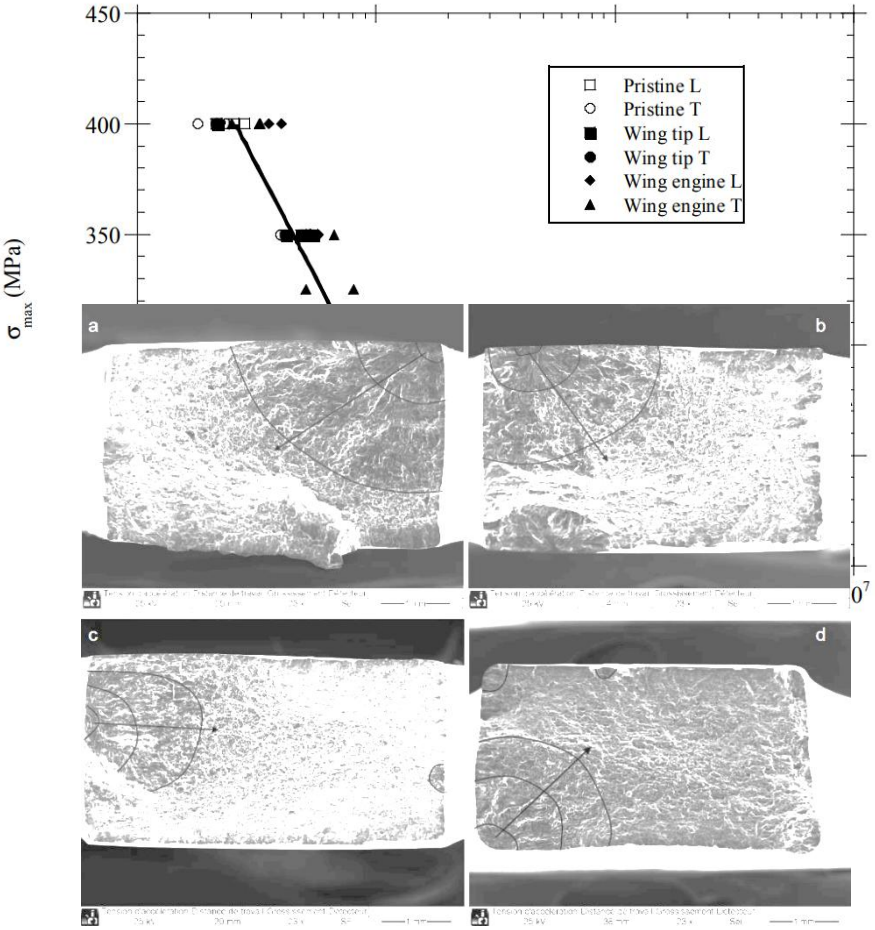

were typically found on flat surfaces, edges, or corners of the specimen cross-section. Figure 4 presents representative examples of crack initiation regions observed at different stress levels in both new and aged materials. In several instances, multiple initiation sites were observed on a single fracture surface, as depicted in Figures 4(c) and 4(d). Additionally, crack initiation was found to occur at different positions along the gage section of the specimens. In some cases, such as that illustrated in Figure 4(b), multiple crack fronts coalesced during final failure. In this example, the primary crack originated in the upper left corner on the front face of the specimen, propagated, and ultimately merged with another crack that had initiated on a parallel plane, resulting in a shear band formation visible in the lower left area of the image.

eISSN: 2349-5715 pISSN: 2349-5707

Volume: 12, Issue 05, May-2025 SJIF 2019: 4.702 2020: 4.737 2021: 5.071 2022: 4.919 2023: 6.980 2024: 7,662

Fig. 3: Normalized S-N curves expressed as the ratio of maximum stress to ultimate tensile stress as a function of the number of cycles to failure.

Fig. 4: SEM observations of fracture surfaces in some specimens obtained from the parent material at 250 MPa (a) and 300 MPa (b), the extreme wing material at 300 MPa (c) and the wing "engine" material at 400 MPa (d).

Analysis of the fracture surfaces further reveals that the crack propagation stage constitutes a major portion of the overall fatigue life. This observation is supported by simulations using AFGROW software, applying the NASGRO equation for the 2024-T351 alloy, as well as by experimental determination of initial defect sizes—either directly measured or estimated using the Equivalent Initial Flaw Size (EIFS) method [7]. The crack growth phase is marked by features indicative of quasi-cleavage fracture and dimple rupture. Faceted regions are also commonly observed on the fracture surfaces, as illustrated in Figures 5 and 6. These facets bear resemblance to Stage I crack growth behavior [8]. Their crystallographic origin was confirmed through etching, which revealed pitting patterns; as shown in Figure 6(c), the triangular pits suggest localized crack growth along {111} planes. Nevertheless, the widespread presence of these facets, sometimes located far from the initiation site, implies that they are not exclusively linked to subsurface crack initiation. Furthermore, such facets appeared in all three types of materials investigated, and no consistent relationship was found between their occurrence—whether in terms of number, distribution, or surface area—and the

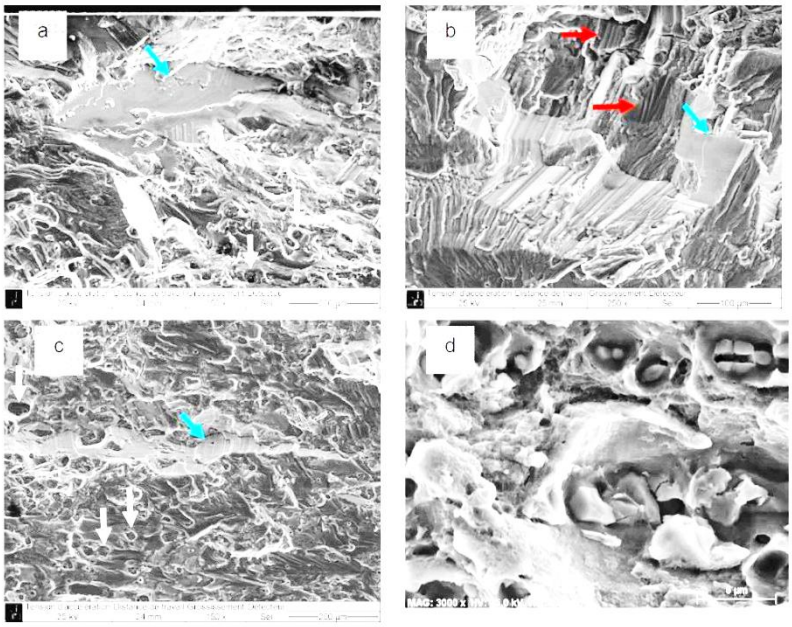

material type. Fracture surfaces also exhibited multiple regions with visible fatigue striations [9,10], as shown in Figure 7. Measurements of striation spacing were performed on specimens from the new material, the wing tip, and the engine-adjacent wing zone. Typically, the spacing ranged between 10^{-7} and 10^{-6} meters, with wider spacing—and thus higher crack growth rates—observed further from the

eISSN: 2349-5715 pISSN: 2349-5707

Volume: 12, Issue 05, May-2025 SJIF 2019: 4.702 2020: 4.737 2021: 5.071 2022: 4.919 2023: 6.980 2024: 7,662

initial crack origin.

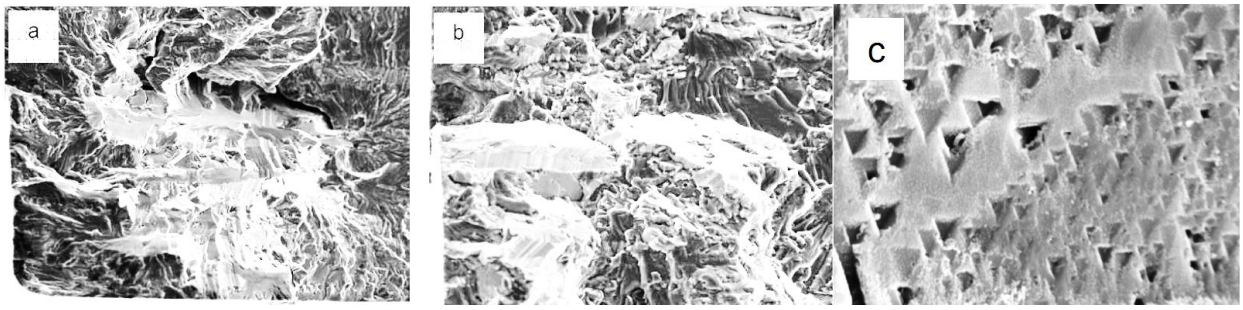

Fig. 5: Observations of the primary material distribution zones at 250 (a) and 300 MPa (b), the engine area made of wing material at 275 MPa (c) and the wingtip material at 250 MPa - Pits at high magnification (d) (vertical white arrows: pits; To assess the potential impact of real-world aging on fatigue crack growth resistance, tests were performed on materials taken from the wing tip and the area near the engine. Figures 8 and 9 display the respective results, alongside data for the new (unaged) material. These experimental findings were also compared with theoretical predictions based on the NASGRO equation for the 2024-T351 aluminum alloy [11].

Fatigue Crack Growth Resistance

While some discrepancies were observed between the experimental data and the NASGRO model—particularly at higher crack growth rates—this behavior is consistent with prior observations by Schörring and Grandt [3]. Notably, both the engine-area material and the new material show similar levels of deviation, whereas the wing tip material aligns more closely with the NASGRO prediction. The comparable crack growth performance between the aged and new materials supports the S–N curve data, which indicate that most of the fatigue life is spent in the crack propagation phase. Moreover, no significant differences in fatigue strength were detected, suggesting that aging in the engine-adjacent region has minimal influence on crack growth resistance. These results are in agreement with the findings reported by Everett [2], but differ from those of Nesterenko et al. [12], who documented a 1.5–4 fold increase in crack growth rate and a reduction in fatigue strength, despite the yield strength and elongation values remaining within the original design specifications.

Conclusion

The investigation of the fatigue strength of 2024 T351 aluminum alloy taken from the wing of a retired A320 aircraft showed no significant differences when compared to the new alloy. Specifically, the fatigue life, crack growth rates, and fracture modes were comparable, despite the wing material experiencing hardening due to aging, particularly near the engine area. However, since these findings are based on only one wing, more data are required to draw statistically reliable conclusions about the impact of aging on fatigue performance. Future studies should also aim to evaluate fatigue behavior under more realistic loading scenarios, reflecting the actual load spectrum experienced by the wing.

Literatures:

1. D. G. Harlow and R. P. Wei, Materials ageing and structural reliability, Int. Journ. of Mat. & Product Techn. 16 (2001) 304-316.
2. R. A. Everett, Effects of service usage on tensile, fatigue and fracture properties of 7075-T6 and 7178-T6 aluminium alloys, NASA Langley Research Center, Hampton, Va (1975).

eISSN: 2349-5715 pISSN: 2349-5707

Volume: 12, Issue 05, May-2025 SJIF 2019: 4.702 2020: 4.737 2021: 5.071 2022: 4.919 2023: 6.980 2024: 7,662

3. J. N. Scheuring and A. F. Grandt, Mechanical properties of aircraft materials subjected to long periods of service usage, Jour. of Eng. Mat. and Techn.-Trans. of the Asme 119 (1997) 380-386.
4. J. J. Gruff and J. G. Hutcheson, Effects of corrosive environments on fatigue life of aluminium alloys under maneuver spectrum loading, Defense Technical Information Centre (1969).
5. F. Menan and G. Henaff, Influence of frequency and waveform on corrosion fatigue crack propagation in the 2024-T351 aluminium alloy in the S-L orientation, Mat. Sc. & Eng.: A 519 (2009) 70-76.
6. F. Menan and G. Henaff, Influence of frequency and exposure to a saline solution on the corrosion fatigue crack growth behavior of the aluminum alloy 2024, Int. Journ. of Fat. 31 (2009) 1684-1695.
7. F. Billy. Vieillissement et propriétés résiduelles de matériaux issus du démantèlement d'avions en fin de vie, PhD., ISAE-ENSMA, Poitiers (2013).
8. J. Petit, Some aspects of near-threshold fatigue crack growth: microstructural and environmental effects, Fatigue Crack Growth Tresholds Concepts, TMS,Philadelphia, Pa, D.L. Davidson and S. Suresh Eds, 3-25 (1983).
9. C. Laird and G. C. Smith, Crack propagation in high stress fatigue, Phil. Mag. 7 (1962) 847- 857.
10. R. M. N. Pelloux, Crack Extension by Alternate Shear, Eng. Fract. Mech. 1 (1970) 697-704.
11. NASGRO, NASGRO Fracture Mechanics and Fatigue Crack Growth Analysis Software. (2002), NASA,Southwest Research Institute: San Antonio, TX (2002).
12. G. I. Nesterenko, V. N. Basov, B. G. Nesterenko, and V. G. Petrusenko, How long time exploitation of the airplanes influences on airplane materials and structures properties, Journal of Machinery and Reliability 4 (2006) 330-337.
13. Дустмуродов Э. Э., Махмудова Д. Х., Юркевич Н. П. Образование частиц при релятивистском столкновении тяжелых ядер на LHC с помощью GEANT4. – 2023.
14. Дустмуродов Э. Э., Махмудова Д. Х., Дустмуродова Х. Э. Обзор современного оборудования. – 2024.
15. Дустмуродов Э. Э. и др. МОДЕЛИРОВАНИЕ ДНК С ИСПОЛЬЗОВАНИЕМ GEANT4 //Eurasian Journal of Technology and Innovation. – 2024. – Т. 2. – №. 6. – С. 26-36.
16. Klychev S. I. et al. A Procedure for Calculating the Heating Temperatures of Flat Transparent Screens for Solar Power Plants //Applied Solar Energy. – 2022. – Т. 58. – №. 2. – С. 259-263.